AGU100 ADVANCING EARTH AND SPACE SCIENCE

Geophysical Research Letters

RESEARCH LETTER
10.1029/2019GL082687

Steve: The Optical Signature of Intense Subauroral Ion Drifts

W. E. Archer[1], B. Gallardo-Lacourt[2], G. W. Perry[2,3], J. P. St.-Maurice[1,4], S. C. Buchert[4,5], and E. Donovan[2]

[1]Department of Physics and Engineering Physics, University of Saskatchewan, Saskatoon, Saskatchewan, Canada, [2]Department of Physics and Astronomy, University of Calgary, Calgary, Alberta, Canada, [3]Center for Solar-Terrestrial Research, New Jersey Institute of Technology, Newark, NJ, USA, [4]Department of Physics and Astronomy, University of Western Ontario, London, Ontario, Canada, [5]Swedish Institute of Space Physics, Uppsala, Sweden

Abstract Little is currently known about the optical phenomenon known as Steve. The first scientific publication on the subject suggests that Steve is associated with an intense subauroral ion drift (SAID). However, additional inquiry is warranted as this suggested relationship as it is based on a single case study. Here we present eight occurrences of Steve with coincident or near-coincident measurements from the European Space Agency's Swarm satellites and show that Steve is consistently associated with SAID. When satellite observations coincident with Steve are compared to that of typical SAID, we find the SAID associated with Steve to have above average peak ion velocities and electron temperatures, as well as extremely low plasma densities.

Key Points:
- Eight Steve events were identified in all-sky imager measurements with coincident or near-coincident measurements from the Swarm satellites
- In all cases, evidence of subauroral ion drifts are observed in Swarm measurements
- All measurements of SAID overlapping with Steve have very fast ion flows, high electron temperatures, and extremely low plasma densities

Supporting Information:
- Supporting Information S1

Correspondence to:
W. E. Archer,
wea784@mail.usask.ca

Citation:
Archer, W. E., Gallardo-Lacourt, B., Perry, G. W., St.-Maurice, J.-P., Buchert, S. C., & Donovan, E. F. (2019). Steve: The optical signature of intense subauroral ion drifts. *Geophysical Research Letters*, *46*, 6279–6286. https://doi.org/10.1029/2019GL082687

Received 4 MAR 2019
Accepted 28 MAY 2019
Accepted article online 4 JUN 2019
Published online 26 JUN 2019

1. Introduction

A new optical phenomenon has recently been brought to the attention of the space physics community by auroral photographers. Steve is observed as a latitudinally narrow, longitudinally extended purple band of light equatorward of the auroral oval. MacDonald et al. (2018) presented the first scientific report of Steve, and investigated the phenomenon simultaneously with a ground-based all-sky imager (ASI), photographs taken by citizen scientists, and in situ measurements from the European Space Agency's Swarm A satellite. These observations showed the optical signature of Steve to be roughly colocated with a subauroral ion drift (SAID). Typical of SAID, this event was located at the equatorward edge of the premidnight region 2 (R2) downward current system in the midlatitude density trough. MacDonald et al. (2018) also reported that the SAID associated with Steve was unusually intense. These initial results show Steve to be a subauroral phenomenon, and as it was measured within a region of weak downward field-aligned current (FAC), unlikely to be caused by precipitating electrons. This result was supported by Gallardo-Lacourt et al. (2018) who present particle measurements from Polar Orbiting Environmental Satellite coincident with an occurrence of Steve identified in ASI measurements. They reported an absence of precipitating charged particles coincident with the optical signature of Steve. In these previous studies, the name “Steve" was presented as the acronym for Strong Thermal Emission Velocity Enhancement. As the physical mechanisms responsible for this phenomenon have not yet been established, in this study we will simply refer to it as Steve.

What then is known about the physical mechanisms for Steve? Gallardo-Lacourt et al. (2018) suggested an ionospheric source for the optical phenomenon, as opposed to magnetospheric precipitating particles responsible for aurora. The results of MacDonald et al. (2018) suggested an association between SAID and Steve. Some characteristics of SAID may be responsible for Steve, or these two phenomena may share a generation mechanism. However, MacDonald et al. (2018) presented a single case study. Therefore, we cannot confidently state that Steve is consistently associated with SAID or that those SAID are unusually intense. In this study we present seven additional occurrences of Steve (as well as the event presented by MacDonald et al., 2018) identified in ASI measurements with near-coincident in situ measurements from the Swarm satellite mission. We show that in all cases, there is evidence of SAID associated with Steve. Furthermore, we determine that for the cases when Swarm satellites passed directly above Steve, they measured extreme plasma parameters relative to most SAID. These observations suggest that the case study presented by MacDonald et al. (2018) is representative of a consistent association between intense SAID and Steve.

SAID initially form near the poleward edge of the midlatitude density trough during geomagnetically active conditions (Spiro et al., 1978). SAID are associated with very little Pedersen current (compared to the auroral zone) and can have flows of several kilometers per second due to the low conductivity of the midlatitude trough. The accepted view of the trough during geomagnetically quiet conditions is that the combination of the dawn-dusk and the corotation electric fields results in a region of stagnation in darkness, allowing recombination to result in a region of relatively low plasma density, n_e (Brinton et al., 1978). The electron temperature, T_e, within the trough is typically anticorrelated with plasma density. This anticorrelation has often been described in terms of a relatively evenly distributed topside electron heat flux acting on regions with different plasma density. Regions of lower n_e have higher T_e as lower plasma densities result in greater thermal energy available per electron. During active conditions, the fast flows of SAID can further decrease the density in the trough through increased production of NO^+, which quickly dissociatively recombines (Schunk et al., 1976). Anderson et al. (1991) report significant NO^+ concentrations around 250-km altitude associated with SAID. See Moffett and Quegan (1983) for a more in-depth description of the midlatitude density trough. Richards et al. (2014) suggested an additional mechanism for generating the trough during geomagnetically active conditions. They presented observations of a summertime trough around 21 MLT that is difficult to explain through convection stagnation as most of the high-latitude region remains sunlit at this time. Richards et al. (2014) proposed that the observed trough was caused by plasma that had previously been corotating with the Earth in darkness before being drawn sunward by an expanding convection pattern.

Several optical signatures have been previously reported in the subauroral region. Pedersen et al. (2007) reported feint optical structures as far as 10° equatorward of the traditional auroral oval. This phenomena seem to be different from Steve as they are associated with kiloelectronvolt electron precipitation and are described as "highly structured." Stable auroral red (SAR) arcs are likely the subauroral optical phenomena that have been most thoroughly studied. They form in the midlatitude density trough when temperatures exceed 3500 K presumably by electron heat conduction from the magnetosphere that has been enhanced by interactions between the ring current and plasmaspheric electrons during geomagnetic storms (Fok et al., 1993; Thorne & Horne, 1992). At these temperatures there are sufficient high-energy electrons among the thermal population to excite SAR arcs (Cole, 1965; Kozyra et al., 1990). Foster et al. (1994) observed a SAR arc to be coincident with an ion drift of ~500 m/s in the midlatitude density trough during a geomagnetic storm. SAR arcs have a mean duration of 10 hr, have a typical latitudinal width of 500 km, and radiate in red at 630 nm (see ; Kozyra & Nagy, 1997, and references therein). Khalipov et al. (2001) suggested that some of the SAR arcs presented in the literature are connected to SAID and are not "classical" SAR arcs and reported weak (subvisual) optical signatures associated with SAID. Sazykin et al. (2002) presented a model description of this optical signature and found that like SAR arcs, hot thermal electrons colocated with SAID could contribute significantly to the observed optical signature. However, unlike SAR arcs, Sazykin et al. (2002) show that ion-neutral frictional heating could also significantly contribute to the observed optical emissions due to the large ion velocities associated with SAID. In this study we will present Swarm satellite measurements coincident with multiple occurrences of Steve to solidify the relationship between SAID and Steve and to provide in situ observations to constrain possible generation mechanisms of Steve.

2. Methodology

The optical measurements presented in this study are from the Time History of Events and Macroscale Interactions during Substorm (THEMIS) and the Redline Geospace Observatory (REGO) ASI arrays. The THEMIS ASIs are while light CCD imagers, each with a temporal resolution of 3 s and a spatial resolution of ~100 m near the zenith. For more information on the THEMIS ASI, see Donovan et al. (2006) and Mende et al. (2008). The REGO imagers are sensitive to wavelengths between ~628 and 632 nm, each with a temporal resolution of 3 s, and a spatial resolution of ~1.5 km near the zenith. For more information on the REGO ASI, see Liang et al. (2016) and Gillies et al. (2017). For this study Steve events were identified as a narrow band of emissions immediately equatorward of and separated from the auroral oval; many of these events are those presented by Gallardo-Lacourt et al. (2018). Using both the THEMIS ASI and REGO data sets, we identified 33 occurrences of Steve. Of these, 23 events were identified in THEMIS ASI observations from December 2007 to December 2015, and 10 events were identified in REGO ASI observations from November 2014 to October 2018. It should be noted that while a purple color is a defining feature of Steve when observed with the naked eye, many of the optical measurements in this study are made with REGO imagers (only sensitive to red light).

The Swarm satellites passed within 2 hr MLT of 8 of the 33 occurrences of Steve identified in optical measurements, providing in situ ionospheric measurements near Steve. The measurements from the satellites are well suited for the study of ionospheric subauroral phenomena. Their polar orbits precess through all magnetic local time every 4.5 months and the midlatitude density trough can often be identified at Swarm altitudes (between 450 and 500 km; Yizengaw & Moldwin, 2005). The Swarm satellites measure electric and magnetic fields, as well as electron density and temperature; see Jørgensen et al. (2008) and Knudsen et al. (2017) for more information on the Swarm instrument package. Plasma density and electron temperature measurements are from the Langmuir probe (LP) extended data set. Ion velocity, $\mathbf{v_i}$, measurements presented in this study are from the 16-Hz thermal ion imager cross-track data set. FAC measurements presented in this study are based on single-satellite magnetometer measurements and assume that the satellites are passing through infinite sheets of current. In this study we present measurements from all three Swarm satellites, which implies that the satellites are all calibrated to one another. While a direct intersatellite comparison has not been done for the Swarm satellites, scientific publications using multiple Swarm satellites (Archer et al., 2015; Goodwin et al., 2015; Spicher et al., 2015) as well as validation studies (Lomidze et al., 2017, 2019) all show the Swarm satellites to behave similarly to one another.

In order to directly compare ground-based optical to in situ satellite measurements, we mapped the geographic position of the Swarm satellites down to 230-km altitude, following International Geomagnetic Reference Field magnetic field lines. We did this using a fixed-step, leapfrog method described in Kouznetsov and Knudsen (2013). All coincident optical measurements in this study are from REGO, which we mapped to 230-km altitude. This is the typical altitude red line emissions are mapped to (Gillies et al., 2017). We identified the window of time that the magnetic footprint of the Swarm satellites spent colocated with the optical signature of Steve to estimate the location of Steve relative to measurements made by the Swarm satellites. A sample ASI image with satellite orbit and estimated location of Steve overlaid is provided as supporting information.

To provide a standard to which these Steve events can be compared, we identified SAID events in Swarm measurements as velocity peaks exceeding 500 m/s separated spatially from the auroral convection flows and colocated with the midlatitude density trough. This is a typical operational definition of SAID in the absence of particle measurements (Spiro et al., 1978). Between 11 December 2013 (earliest electric field measurements from the mission) and 31 December 2014, 122 SAID events were identified in Swarm A measurements. This time period was selected as it samples all MLT roughly equally, all seasons equally, and there are few gaps in Swarm cross-track plasma flow measurements. These events are ideal for comparison with measurements of Steve as they were made by a single instrument at similar altitudes. A list of their times is available in the supporting information.

In this study we compare SAID and Steve events by the plasma parameters measurements provided by the Swarm satellites. We compare the extrema of most plasma parameters; namely, maximum v_i, maximum T_e, and minimum n_e. To characterize the modest localized enhancement in downward FAC associated with SAID (He et al., 2016), we integrated FAC over ~30 km surrounding each SAID/Steve event, to estimate the total FAC enhancement of each event.

3. Results

3.1. Steve Measurements With Swarm

At the time of this study 33 occurrences of Steve have been identified in scientific optical measurements. Of those events, a Swarm satellite passed directly above or near Steve on eight occasions. Figure 1 shows the plasma parameters measured by the Swarm satellites for all eight events, plotted in altitude-adjusted corrected geomagnetic latitude (MLat). Each crossing is centered on the position at which the maximum electron temperature was measured within the midlatitude density trough. Event c corresponds to the occurrence of Steve presented by MacDonald et al. (2018). The LP measurements presented in this study are superficially different than those presented by MacDonald et al. (2018), as they were processed by a more recent algorithm. In cases where Swarm passed directly above Steve within the field of view of an ASI, the approximate location of Steve is shown as a gray-shaded box in Figure 1. The optical signature of Steve is very faint in most cases, and these shaded areas only roughly mark the boundaries of Steve and are as such significantly wider than the average full width at half maximum of ~20 km reported by Gallardo-Lacourt et al. (2018). For event e, at the time that Swarm C passed through the field of view of the ASI, its orbit was roughly 0.8 h west of the westmost extent of Steve. Steve then expanded eastward along the equatorward

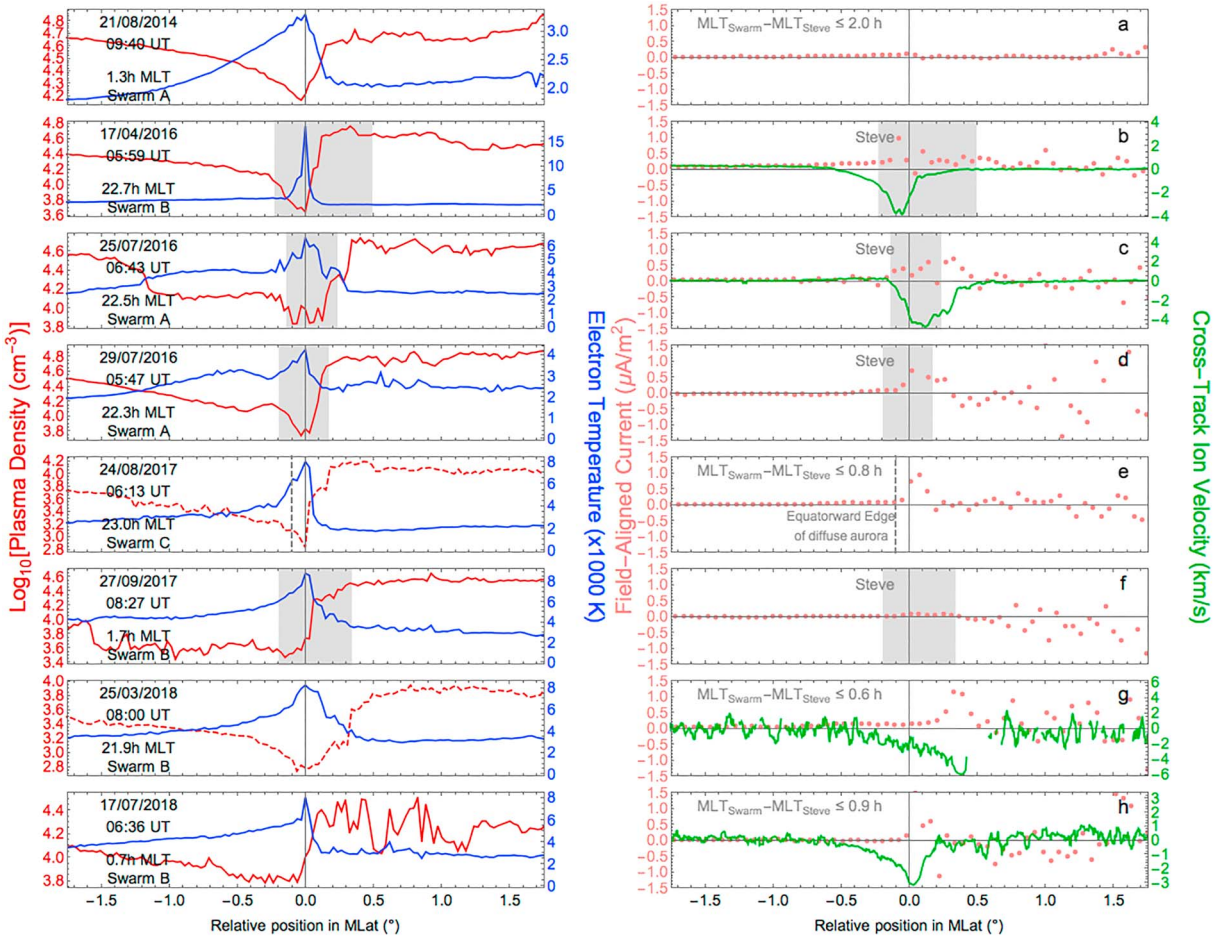

Figure 1. Plasma density and electron temperature (left panels) and field-aligned current and ion velocity (right panels) measured by Swarm satellites passing near/through Steve events that had been identified in all-sky imager measurements for eight events. Plasma density is shown in red with solid lines estimated from Langmuir probed ion current and dashed lines estimated from electron current. Electron temperature is shown in blue. Field-aligned current is shown in pink. Cross-track ion velocity is shown in green. Location of Steve along the satellite track is shaded in gray. The equatorward edge of the diffuse aurora is marked with a dashed gray line for the event e, from 24 August 2017. Steve = Strong Thermal Emission Velocity Enhancement.

edge of the diffuse aurora, reaching the MLT of the Swarm orbit only 2 min after the satellite crossed. A gray dashed line for event e in Figure 1 shows the optical boundary of the diffuse aurora (where Steve forms 2 min after the Swarm crossing). In events a, g, and h, conditions were cloudy directly beneath the Swarm satellites, and so Steve was identified in adjacent ASI. In these cases the MLT difference between Swarm and nearest observed point of Steve (seen at the edge of the closest ASI) is listed in Figure 1. This represents the maximum possible distance between Swarm and Steve as we do not know how far Steve extends beyond the field of view of the cameras and can span over 2,000 km in latitude (Gallardo-Lacourt et al., 2018). At the latitudes of the observations presented in Figure 1 near the surface of the Earth, 1 hr of MLT corresponds to roughly 800 km in longitudinal separation. It should be noted that ion velocity measurements are only available in four cases, as the Swarm electric field instrument (EFI) was not operating for the other events. Also, for the Swarm mission n_e is typically derived from LP ion current (measured at negative probe bias). Plasma density is often derived from ion rather than electron saturation current, as it is independent of electron temperature. However, in a few cases this n_e reached negative values, possibly because of inaccurately calibrated electronic offsets. In those cases, n_e is instead estimated from LP electron current and is shown as a dashed red line (rather than a solid one) in Figure 1.

For all cases in Figure 1, a clear midlatitude density trough is observed in Swarm measurements, with a peak in T_e (shown in blue) roughly colocated with the minimum in n_e (shown in red). The FAC (shown in pink) when crossing the point of maximum T_e for all cases was either positive, indicating a downward FAC, or near zero. Narrow channels of enhanced westward ion velocity (shown in green) were also observed roughly

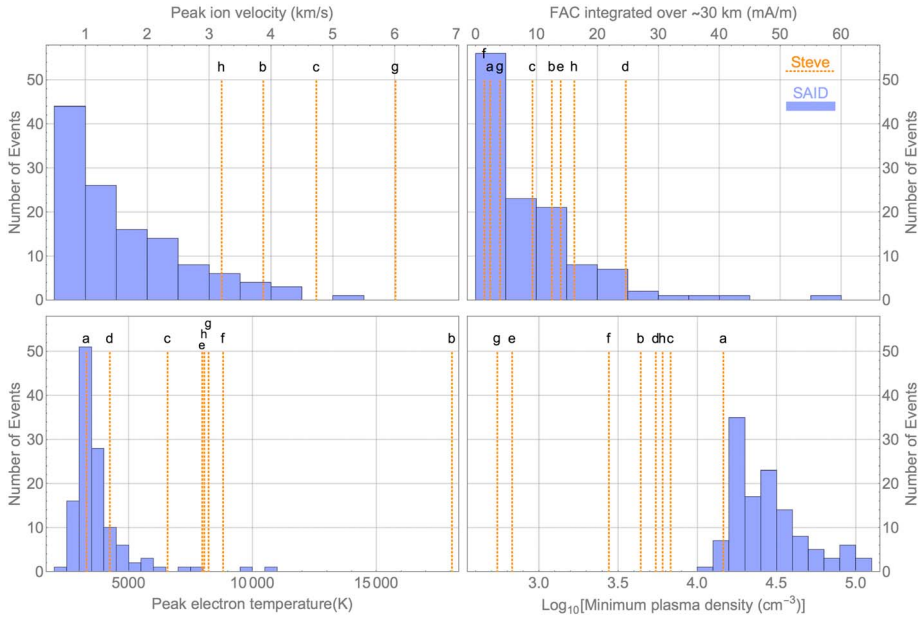

Figure 2. Histograms of (top left) plasma peak ion velocity, (top right) field-aligned current integrated over 30 km, (bottom left) peak electron temperature, and (bottom right) minimum plasma density measured by the Swarm A satellite coincident with 122 SAID events identified between 11 December 2013 and 31 December 2014. Plasma parameters measured coincident with Steve events shown as red dashed lines on histograms. SAID = subauroral ion drift; Steve = Strong Thermal Emission Velocity Enhancement.

colocated with the minimum n_e for all cases in which the Swarm EFI was operating. The EFI was turned on shortly after event a, and a 800-m/s flow channel was observed coincident with the midlatitude density trough on the subsequent orbit (1.5 hr later). It should be noted that because there are no v_i measurements available for four of the events in Figure 1, they do not meet the criteria used in this study to identify SAID. However, in all cases the available Swarm measurements presented in Figure 1 match typical past SAID observations from ~500 km altitude (Anderson et al., 1991; Archer & Knudsen, 2018; Spiro et al., 1979), and are all roughly colocated with occurrences of Steve. We also note that while SAID are reported between 16 and 2 hr MLT with the highest occurrence probability density around 22 MLT (He et al., 2014; Spiro et al., 1979), all Steve events presented so far have been between 22 and 2 MLT.

The observations shown in Figure 1 are qualitatively very similar to those presented by Foster et al. (1994) coincident with a SAR arc. The peak flow enhancement observed by Foster et al. (1994) was ~500 m/s and filled the midlatitude density trough and was accompanied by a peak electron temperature of ~4000 K. Prölss (2006) showed subauroral T_e enhancements of about 3000 K using the LP on the DE-2 satellite. Contrasting these observations, the narrower flow channels situated at the poleward edge of the trough in Figure 1 have peak velocities of several kilometers per second and are colocated with peak electron temperatures ranging from 4000 K to over 10000 K. To provide context for the magnitude of these values, in the next section we establish what is typically observed by the Swarm satellites when crossing SAID.

3.2. Comparing Steve to Typical SAID

We identified 122 SAID events exceeding 500 m/s in peak v_i in Swarm A measurements, which we use to represent typical plasma parameters for SAID when measured from Swarm altitudes. Figure 2 shows histograms of the peak v_i, peak T_e, minimum n_e, and integrated FAC (over ~30 km) for all 122 events. Superposed on these histograms are orange vertical dashed lines, representing the plasma parameters measured by the Swarm satellites that passed through (or near to) Steve. The measurements associated with Steve events have been labeled with lower case letters matching the labels in Figure 1.

Figure 2 shows the majority of SAID to have a FAC integrated over 30 km of less than 10 mA/m. The integrated FAC for the Steve events do not clearly fit nor do they clearly deviate from the distribution established by SAID. The Steve events do, however, clearly deviate from typical SAID in v_i, T_e, and n_e. SAID ion velocities in Figure 2 are most frequently less than 500 m/s, with a median velocity of ≈1.3 km/s. The SAID coincident with Steve events shown in Figure 2 have ion velocities exceeding 3 km/s and are all in the top 5th

percentile relative to typical SAID. Similarly, the peak T_e of six of the eight Steve events in Figure 2 are in the top 3% of peak T_e of SAID. Most striking perhaps is n_e, where the minimum n_e for all Steve events except one are less than any measured for typical SAID. It should be noted that satellite observations for event a, which has relatively low v_i and T_e, as well as relatively high n_e, were taken the farthest from the ASI field of view detecting Steve among events presented in this study. This analysis is limited by the small number of observations of Steve. However, a clear pattern emerges in which Steve is consistently associated with intense SAID with unusually large v_i, high T_e, and extremely low n_e.

4. Discussion and Conclusion

The first scientific publication on Steve (MacDonald et al., 2018) showed the phenomenon to be colocated with an intense SAID. This association between Steve and SAID was based on a single event. We have expanded on the work of MacDonald et al. (2018) by identifying eight occurrences of Steve with coincident or near-coincident Swarm satellite measurements. In all cases, Steve is observed roughly colocated with the minimum n_e and corresponding maximum T_e of the midlatitude density trough. We observe a narrow westward flow channel, consistent with a SAID, for all cases that Swarm ion velocity measurements are available. We found no counter examples to this trend. In other words, for every Swarm crossing near Steve, measurements consistent with SAID were observed. Additionally, these events are intense relative to the average SAID with large v_i, high T_e, and low n_e. How then, does this inform us on the generation mechanism of Steve?

It is clear from REGO observations that Steve radiates in red frequencies. The T_e and v_i measured coincident with Steve are both significantly higher than the values modeled by Sazykin et al. (2002), suggesting that electron impact and ion-neutral frictional heating may both contribute to the red emissions of Steve. The spectral properties of Steve are currently unknown, but a purple glow appears to be a persistent feature. The purple observed in traditional aurora is caused by the deexcitation of N_2^+. However, the optical signature of Steve appears to originate around 230 km, significantly higher altitudes than we expect N_2^+ emissions (Måseide, 1967). The purple appearance of Steve could be due to either violet emissions or a mixture of red with other emissions such as the green line and/or blue line emissions at 557.7 and 427.8 nm with the minimum excitation energies of about 4.2 and 18.8 eV, respectively. If electron impact is responsible for such emissions within Steve, a population of suprathermal electrons is required significantly beyond that of the Maxwellian tail of the heated thermal electrons in order that the brightness of these emissions be comparable with the red line emission. The presence of such suprathermal electrons in SAID events has been reported from Defense Meteorological Satellite Program (DMSP) observations in the topside ionosphere and Combined Release and Radiation Effects Satellite (CRRES), Time History of Events and Macroscale Interactions during Substorms (THEMIS), Van Allen Probes (VAP), and Polar observations in the conjugate plasmasphere (e.g., Mishin, 2013; Mishin et al., 2017).

The extrema in T_e and v_i associated with SAID are often roughly colocated; they are not exactly colocated. This significant distinction is discussed by Moffett et al. (1998), and in this study is most evident for Case g in Figure 1. Unfortunately, the in situ and ground-based observations for Case g were not perfectly coincident, as they may have otherwise shed light on the relative importance of elevated T_e and v_i on the formation of Steve. On a similar note, we must keep in mind that the in situ observations from the Swarm satellites are well above the emission altitudes of Steve. While the latitudinal profiles of v_i presumably map down magnetic field lines, the latitudinal profiles of T_e and n_e will vary with altitude. As such, directly comparing the latitudinal profiles of optical emission, T_e, and v_i at Swarm altitudes will not perfectly reflect what is occuring at Steve emission altitudes.

Several key observations of Steve are still required before a proper simulation of the phenomenon can be carried out. Specifically, the spectral characteristics Steve and altitude range at which it occurs has yet to be determined, and would greatly constrain models of Steve. Regardless of the specific mechanisms responsible for Steve, the observations presented in this study suggest Steve to be the optical signature of exceptionally intense SAID.

Acknowledgments
This study is based on Level 1B and Level 2 Swarm data available at https://earth.esa.int/web/guest/swarm/ data access. Swarm is a project of the European Space Agency. The entire LP density estimates using the electron current are not yet included in the extended LP data set but will be in the next version. The LP currents and n_e estimates used in this work are made available at https://www.space.irfu.se/steve/. Login and password are provided by S. Buchert upon request. William Archer was supported by grants from the European Space Agency and the Natural Sciences and Engineering Council of Canada. The ASI data used in this study were produced with funding from the Canadian Space Agency and National Science Foundation. THEMIS ASI data can be viewed via the University of Calgary data portal located at http://data-portal.phys.ucalgary.ca/. We would like to thank Alexei Kouznetsov for his software used to trace IGRF12 magnetic field lines.

References

Anderson, P. C., Heelis, R. A., & Hanson, W. B. (1991). The ionospheric signatures of rapid subauroral ion drifts. *Journal of Geophysical Research*, *96*(90), 5785–5792. https://doi.org/10.1029/90JA02651

Archer, W. E., & Knudsen, D. J. (2018). Distinguishing subauroral ion drifts from Birkeland current boundary flows. *Journal of Geophysical Research: Space Physics*, *2016*, 819–826. https://doi.org/10.1002/2017JA024577

Archer, W. E., Knudsen, D. J., Burchill, J. K., Patrick, M. R., & St.-Maurice, J.-P. (2015). Anisotropic core ion temperatures associated with strong zonal flows and upflows. *Geophysical Research Letters*, *42*, 981–986. https://doi.org/10.1002/2014GL062695

Brinton, H. C., Grebowsky, J. M., & Brace, L. H. (1978). The high-latitude winter *F* region at 300 km: Thermal plasma observations from AE-C. *Journal of Geophysical Research*, *83*(A10), 4767–4776. https://doi.org/10.1029/JA083iA10p04767

Cole, K. D. (1965). Stable auroral red arcs, sinks for energy of Dst main phase. *Journal of Geophysical Research*, *70*(7), 1689–1706. https://doi.org/10.1029/JZ070i007p01689

Donovan, E., Mende, S., Jackel, B., Frey, H., Syrjäsuo, M., Voronkov, I., et al. (2006). The THEMIS all-sky imaging array-system design and initial results from the prototype imager. *Journal of Atmospheric and Solar-Terrestrial Physics*, *68*(13), 1472–1487. https://doi.org/10.1016/j.jastp.2005.03.027

Fok, M.-C., Kozyra, J. U., Nagy, A. F., Rasmussen, C. E., & Khazanov, G. V. (1993). Decay of equatorial ring current ions and associated aeronomical consequences. *Journal of Geophysical Research*, *98*(1), 19,381–19,393.

Foster, J. C., Buonsanto, M. J., Mendillo, M., Nottingham, D., Rich, F. J., & Denig, W. (1994). Coordinated stable auroral red arc observations: Relationship to plasma convection. *Journal of Geophysical Research*, *99*(A6), 11,429–11,439. https://doi.org/10.1029/93JA03140

Gallardo-Lacourt, B., Liang, J., Nishimura, Y., & Donovan, E. (2018). On the origin of STEVE: Particle precipitation or ionospheric skyglow? *Geophysical Research Letters*, *45*, 7968–7973. https://doi.org/10.1029/2018GL078509

Gallardo-Lacourt, B., Nishimura, Y., Donovan, E., Gillies, D. M., Perry, G. W., Archer, W. E., et al. (2018). A statistical analysis of STEVE. *Journal of Geophysical Research: Space Physics*, *123*, 9893–9905. https://doi.org/10.1029/2018JA025368

Gillies, D. M., Knudsen, D., Donovan, E., Jackel, B., Gillies, R., & Spanswick, E. (2017). Identifying the 630 nm auroral arc emission height: A comparison of the triangulation, FAC profile, and electron density methods. *Journal of Geophysical Research: Space Physics*, *122*, 8181–8197. https://doi.org/10.1002/2016JA023758

Goodwin, L. V., Iserhienrhien, B., Miles, D. M., Patra, S., Meeren, C. V. D., Buchert, S. C., et al. (2015). Swarm in situ observations of *F* region polar cap patches created by cusp precipitation. *Geophysical Research Letters*, *42*, 996–1003. https://doi.org/10.1002/2014GL062610. High-resolution.

He, F., Zhang, X. X., & Chen, B. (2014). Solar cycle, seasonal, and diurnal variations of subauroral ion drifts: Statistical results. *Journal of Geophysical Research: Space Physics*, *120*, 5009–5021. https://doi.org/10.1002/2015JA021023. Received.

He, F., Zhang, X. X., Wang, W., & Chen, B. (2016). Double-peak subauroral ion drifts (DSAIDs). *Geophysical Research Letters*, *43*, 5554–5562. https://doi.org/10.1002/2016GL069133

Jørgensen, J. L., Friis-Christensen, E., Brauer, P., Primdahl, F., Jørgensen, P. S., Allin, T. H., & Denver, T. (2008). The Swarm magnetometry package. In *Small satellites for earth observation* (pp. 143–151). Berlin: Springer.

Khalipov, V. L., Galperin, Y. I., Stepanov, A. E., & Shestakova, L. V. (2001). Formation of a polarization jet during the expansion phase of a substorm : Results of ground-based measurements. *Cosmic Research*, *39*(3), 244–253.

Knudsen, D. J., Burchill, J. K., Buchert, S. C., Eriksson, A., Gill, R., Wahlund, J.-E., et al. (2017). Thermal ion imagers and Langmuir probes in the Swarm electric field instruments. *Journal of Geophysical Research: Space Physics*, *122*, 2655–2673. https://doi.org/10.1002/2016JA022571

Kouznetsov, A., & Knudsen, D. J. (2013). Forward mapping of solar energetic proton distributions through the geomagnetic field. *Journal of Geophysical Research: Space Physics*, *118*, 4724–4738. https://doi.org/10.1002/jgra.50400

Kozyra, J. U., & Nagy, A. F. (1997). High-altitude energy source(s) for stable auroral red arcs. *Reviews of Geophysics*, *25*(96), 155–190.

Kozyra, J. U., Valladares, C. E., Carlson, H. C., Buonsanto, M. J., & Slater, D. W. (1990). Study of the seasonal and solar cycle variations of stable aurora red arcs. *Journal of Geophysical Research*, *95*(A8), 12,219–12,234.

Liang, J., Donovan, E., Jackel, B., Spanswick, E., & Gillies, D. M. (2016). On the 630 nm red-line pulsating aurora: Red-line Emission Geospace Observatory observations and model simulations. *Journal of Geophysical Research: Space Physics*, *121*, 7988–8012. https://doi.org/10.1002/2016JA022901. Received.

Lomidze, L., Burchill, J. K., Knudsen, D. J., Kouznetsov, A., & Weimer, D. R. (2019). Validity study of the Swarm horizontal cross—Ion drift velocities in the high-latitude ionosphere. *Earth and Space Science*, *6*, 411–432. https://doi.org/10.1029/2018EA000546

Lomidze, L., Knudsen, D. J., Burchill, J. K., Kouznetsov, A., & Buchert, S. C. (2017). Calibration and Validation of Swarm plasma densities and electron temperatures using ground-based radars and satellite radio occulation measurements. *Radio Science*, *53*, 15–36. https://doi.org/10.1002/2017RS006415

Måseide, K. (1967). Rocket measurements of the volume profile for auroral glow. *Planetary and Space Science*, *15*, 899–905.

MacDonald, E. A., Donovan, E., Nishimura, Y., Case, N. A., Gillies, D. M., Gallardo-lacourt, B., et al. (2018). New science in plain sight: Citizen scientists lead to the discovery of optical structure in the upper atmosphere. *Science Advances*, *4*(March), 16–21. https://doi.org/10.1126/sciadv.aaq0030

Mende, S. B., Harris, S. E., Frey, H. U., Angelopoulos, V., Russell, C. T., Donovan, E., et al. (2008). The THEMIS array of ground-based observatories for the study of auroral substorms. *Space Science Reviews*, *141*(1-4), 357–387. https://doi.org/10.1007/s11214-008-9380-x

Mishin, E. V. (2013). Interaction of substorm injections with the subauroral geospace : 1. Multispacecraft observations of SAID. *Journal of Geophysical Research: Space Physics*, *118*, 5782–5796. https://doi.org/10.1002/jgra.50548

Mishin, E. V., Nishimura, Y., & Foster, J. (2017). SAPS/SAID revisited: A causal relation to the substorm current wedge. *Journal of Geophysical Research: Space Physics*, *122*, 8516–8535. https://doi.org/10.1002/2017JA024263

Moffett, R. J., Ennis, A. E., Bailey, G. J., Heelis, R. A., & Brace, L. H. (1998). Electron temperatures during rapid subauroral ion drift events. *Annales Geophysicae*, *16*(4), 450. https://doi.org/10.1007/s005850050615

Moffett, R. J., & Quegan, S. (1983). The mid-latitude trough in the electron concentration of the ionospheric *F*-layer: A review of observations and modelling. *Journal of Atmospheric and Terrestrial Physics*, *45*(5), 315–343. https://doi.org/10.1016/S0021-9169(83)80038-5

Pedersen, T., Mishin, E., & Oksavik, K. (2007). Observations of structured optical emissions and particle precipitation equatorward of the traditional auroral oval. *Journal of Geophysical Research*, *112*, 1–14. https://doi.org/10.1029/2007JA012299

Prölss, G. W. (2006). Subauroral electron temperature enhancement in the nighttime ionosphere. *Annales Geophysicae*, *24*, 1871–1885.

Richards, P. G., Nicolls, M. J., St.-Maurice, J. P., Goodwin, L., & Ruohoniemi, J. M. (2014). Investigation of sudden electron density depletions observed in the dusk sector by the Poker Flat, Alaska incoherent scatter radar in summer. *Journal of Geophysical Research A: Space Physics*, *119*, 10,608–10,620. https://doi.org/10.1002/2014JA020541

Sazykin, S., Fejer, B. G., Galperin, Y. I., Zinin, L. V., Grigoriev, S. A., & Mendillo, M. (2002). Polarization jet events and excitation of weak SAR arcs. *Geophysical Research Letters*, *29*(12), 1586. https://doi.org/10.1029/2001GL014388

Schunk, R. W., Banks, P. M., & Raitt, W. J. (1976). Effects of electric fields and other processes upon the nighttime high-latitude *F* layer. *Journal of Geophysical Research*, *81*(19), 3271–3282. https://doi.org/10.1029/JA081i019p03271

Spicher, A., Cameron, T., Grono, E. M., Yakymenko, K. N., Buchert, S. C., Clausen, L. B. N., et al. (2015). Observation of polar cap patches and calculation of gradient drift instability growth times: A Swarm case study. *Geophysical Research Letters*, *42*, 201–206. https://doi.org/10.1002/2014GL062590

Spiro, R. W., Heelis, R. A., & Hanson, W. B. (1978). Ion convection and the formation of the mid-latitude *F* region ionization trough. *Journal of Geophysical Research*, *83*, 4255–4264. https://doi.org/10.1029/JA083iA09p04255

Spiro, R. W., Heelis, R. A., & Hanson, W. B. (1979). Rapid subauroral ion drifts observed by atmosphere explorer C. *Geophysical Research Letters*, *6*(8), 657–660. https://doi.org/10.1029/GL006i008p00657

Thorne, R. M., & Horne, R. B. (1992). The contribution of ion-cyclotron waves to electron heating and SAR-arc excitation near the storm-time plasmapause. *Geophysical Research Letters*, *19*(4), 417–420.

Yizengaw, E., & Moldwin, M. B. (2005). The altitude extension of the mid-latitude trough and its correlation with plasmapause position. *Geophysical Research Letters*, *32*, L09105. https://doi.org/10.1029/2005GL022854